

Enzymatic Reaction of Silent Substrates: Kinetic Theory and Application to the Serine Protease Chymotrypsin

April Case,[‡] W. Phillip Huskey,[§] and Ross L. Stein^{*,‡}

Laboratory for Drug Discovery in Neurodegeneration, Harvard Center for Neurodegeneration and Repair, 65 Landsdowne Street, Fourth Floor, Cambridge, Massachusetts 02139, and Department of Chemistry, Rutgers, The State University of New Jersey, Newark, New Jersey 07102

Received December 31, 2002; Revised Manuscript Received February 20, 2003

ABSTRACT: Investigating the selectivity that an enzyme expresses toward its substrates can be technically challenging if reaction of these substrates is not accompanied by a conveniently monitored change in some physicochemical property. In this paper, we describe a simple method for determining steady-state kinetic parameters for enzymatic turnover of such “silent” substrates. According to this method, silent substrate *S* is allowed to compete for enzymic reaction with signal-generating substrate *S*^{*}, whose conversion to product can be conveniently monitored. Full reaction progress curves are collected under conditions of $[S^*]_0 \ll K_m^*$ and $[S]_0 \geq 3K_m$. Progress curves collected under these conditions are characterized by an initial lag phase of duration τ that is followed by the pseudo-first-order reaction of *S*^{*}. Steady-state kinetic parameters for the silent substrate can be obtained by one of two methods. One method combines least-squares fitting with numerical integration of appropriate rate equations to analyze the progress curves, while the other method relies on direct graphical analysis in which K_m is the value of $[S]_0$ that reduces the control velocity by a factor of 2 and V_{max} is shown to simply equal the ratio $[S]_0/\tau$. We use these methods to analyze the α -chymotrypsin-catalyzed hydrolysis of silent substrate Suc-Ala-Phe-AlaNH₂ with signal generator Suc-Ala-Phe-pNA. From the curve-fitting method, $k_c = 0.9 \pm 0.2$ s⁻¹ and $K_m = 0.4 \pm 0.1$ mM, while by direct graphical analysis, $k_c = 1.1 \pm 0.1$ s⁻¹ and $K_m = 0.51 \pm 0.03$ mM. As validation of this new method, we show agreement of these values with those determined independently by HPLC analysis of the hydrolysis of Suc-Ala-Phe-AlaNH₂ by α -CT, where $k_c = 1.1 \pm 0.1$ s⁻¹ and $K_m = 0.5 \pm 0.1$ mM.

Enzymes bind and react efficiently only with those substrates that possess certain structural features. Identifying these structural features is critical to a full understanding of the enzyme's catalytic properties and is particularly important for enzymes that possess a relatively broad selectivity toward their substrates. Enzymes of broad selectivity can be found among those that act on protein or peptide substrates and include proteases and protein kinases and phosphatases. To probe the substrate selectivity of these enzymes, steady-state kinetic parameters are measured for a series of substrates that are derived from systematic variation of amino acid residues in the neighborhood of the substrate's center of reaction. The dependence of a particular kinetic parameter on substrate structure constitutes a definition of the enzyme's selectivity toward substrate.

Now, the action of protein hydrolases, kinases, or phosphates is not ordinarily accompanied by a conveniently monitored change in a physicochemical property such as absorbance or fluorescence. The lack of an analytical signal that can be readily followed over time represents a significant technical obstacle to the investigation of an enzyme's substrate selectivity and to the investigation of an enzyme's

kinetic properties, in general (1, 2). To circumvent this problem, one option is to develop assays based on separation of product from unreacted substrate, using, for example, high-pressure liquid chromatography. While precise and accurate kinetic constants can often be obtained if one uses semicontinuous methodology coupled with HPLC¹ (3), such analyses are still cumbersome and require specialized automation equipment for sample injection and peak integration. More typically, investigators have modified the structure of the enzyme's natural protein substrate so that reaction of the new substrate is accompanied by a conveniently monitored signal. As a consequence of modification, these new substrates not only will possess additional chemical moieties relative to natural substrates but frequently will have been truncated and, thus, may lack important structural features. For example, in the case of serine proteases, a common strategy has been to first truncate a natural protein substrate to produce a small, synthetically manageable peptide and then to replace the C-terminal half of this peptide with either a chromophoric *p*-nitroaniline or some other chromophoric or fluorogenic leaving group (see Scheme 1). While such a strategy allows the production of a series of substrates for exploration of the “unprimed” side of the scissile bond, no information can be obtained for the “primed” side. In

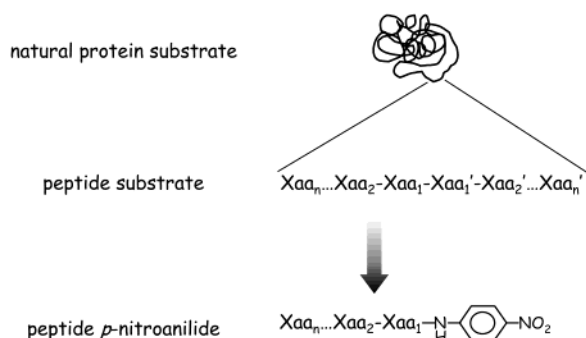
* To whom correspondence should be addressed. Phone: (617) 768-8651. Fax: (617) 768-8606. E-mail: rstein@rics.bwh.harvard.edu.

[‡] Harvard Center for Neurodegeneration and Repair.

[§] Rutgers, The State University of New Jersey.

¹ Abbreviations: Suc, *N*-succinyl; pNA, *p*-nitroanilide; α -CT, α -chymotrypsin; HPLC, high-pressure liquid chromatography.

Scheme 1: Stepwise Development of Convenient Substrates for Serine Protease



addition, such a strategy implicitly assumes that the specificity of peptide *p*-nitroanilides will be the same as the specificity of peptides.

In this paper, we describe a new method for determining steady-state kinetic parameters for enzymatic turnover of “silent” substrates, such as unmodified peptides. According to this method, the silent substrate is allowed to compete for enzymatic reaction with a substrate whose conversion to product can be conveniently monitored. Full reaction progress curves are collected, and steady-state kinetic parameters for the silent substrate are calculated by either curve-fitting methods or by a simple and direct graphical analysis of the progress curves. This method is used to analyze the α -chymotrypsin-catalyzed hydrolysis of silent substrate Suc-Ala-Phe-AlaNH₂ with Suc-Ala-Phe-pNA as the signal generator.

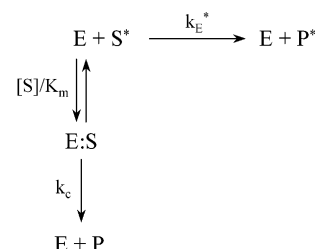
MATERIALS AND METHODS

General. Buffer salts were from Sigma Chemical Co. Suc-Ala-Phe-pNA and Suc-Ala-Phe-AlaNH₂ were purchased from Absolute Science (Cambridge, MA). Bovine α -CT was a crystalline product from Sigma (C 7762) and was used without further purification.

Assay and Reagent Solutions. Assay buffer was a pH 8.0 solution of 50 mM HEPES, 500 mM NaCl, 10 mM CaCl₂, and 1 mM EDTA. Stock solutions (50 and 250 mM) of Suc-Ala-Phe-pNA and Suc-Ala-Phe-AlaNH₂, respectively, were prepared in DMSO. Stock solutions of α -CT were prepared in 1 mM HCl at 2.5 mg/mL ($[\alpha\text{-CT}]_{\text{stock}} = 100 \mu\text{M}$) and stored in 1.0 mL aliquots at -80°C . Each day's kinetic experiments were conducted with a freshly thawed aliquot of stock enzyme.

Kinetic Methods: Continuous Assay for the α -CT-Catalyzed Hydrolysis of Suc-Ala-Phe-AlaNH₂. All reactions were run in the wells of 96-well microtiter plates and read by a computer-interfaced Molecular Devices Spectra Max Plus plate reader. In a typical experiment, appropriate volumes of assay buffer and a solution of 36 mM Suc-Ala-Phe-AlaNH₂ in assay buffer are added to the wells of a plate to achieve a volume of 50 μL . Note that, at this point in the assay, the concentration of Suc-Ala-Phe-AlaNH₂ is twice the final, desired concentration. To each of these wells is then added 50 μL of a 400 μM Suc-Ala-Phe-pNA solution in buffer. Finally, to initiate the reaction, 5 μL of a 100 μM solution of α -CT stock solution is added. Under these conditions, $[\text{Suc-Ala-Phe-AlaNH}_2]_0 \leq 18 \text{ mM}$, $[\text{Suc-Ala-Phe-pNA}]_0 = 200 \mu\text{M}$, $[\alpha\text{-CT}]_0 = 4.7 \mu\text{M}$, and $[\text{DMSO}]_0 = 4\%$. Hydrolysis of Suc-Ala-Phe-pNA is monitored as the absor-

Scheme 2: Mechanism for Reaction of Signal-Generating Substrate S* in the Presence of Competing, Silent Substrate S



bance change at 410 nm that accompanies the production of *p*-nitroaniline at 30°C .

Kinetic Methods: HPLC-Based Assay for the α -CT-Catalyzed Hydrolysis of Suc-Ala-Phe-AlaNH₂. In this assay, aliquots of reaction solutions of α -CT and Suc-Ala-Phe-AlaNH₂ are fractionated by HPLC, and the disappearance of substrate is monitored over time as a reflection of reaction progress. Reaction products are separated from intact substrate by reverse-phase chromatography on a Waters Alliance 2795 HPLC system with UV detection at 210 nm. In a typical kinetic run, a 40 μL aliquot of a reaction mix maintained at 30°C is injected every 11 min onto a Waters C₈ Nova-Pak column that had been equilibrated in 30% AcCN/0.075% TFA. Column elution is isocratic at a flow rate of 1 mL/min. Substrate elutes at 8.3 min, and its peak area is integrated, converted to concentration using a calibration curve, and plotted as a function of time.

Curve Fitting and Simulations. Fitting of progress curves and production of simulations were accomplished using the program Scientist, MicroMath Scientific Software [available through Echoscans, Inc. (<http://www.echoscansinc.com>), P.O. Box 2111, Niagara Falls, Ontario, Canada L2E 672].

RESULTS AND DISCUSSION

Development of Theory. Progress curves for enzymatic turnover of signal-generating substrate S* in the presence of competing silent substrate S contain kinetic information about both reactions. If reactions are run under the initial conditions $[S]_0 \geq K_m$ and $[S^*]_0 \ll K_m^*$, these progress curves will exhibit an initial lag phase of duration τ that is followed by pseudo-first-order turnover of S*. This kinetic mechanism is illustrated in Scheme 2 and simulated in Figure 1. In this scheme, k_E^* corresponds to k_c^*/K_m^* and governs the reaction when $[S^*]_0 \ll K_m^*$.

Several noteworthy points emerge from the simulations of Figure 1: (1) In Figure 1A, it can be seen that the initial velocities of the progress curves decrease with increasing $[S]_0$ and conform to the relationship of eq 1. In eq 1, silent

$$v_o = \frac{k_E^*[E]_0[S^*]_0}{1 + [S]/K_m} = \frac{v_{\text{control}}}{1 + [S]/K_m} \quad (1)$$

substrate S behaves as a competitive inhibitor of the enzyme with the inhibition constant determined as K_m . This feature will allow us to determine K_m values directly from progress curves that are collected under the condition $[S^*]_0 \ll K_m^*$. (2) Figure 1A illustrates that τ increases with increasing $[S]_0$, while Figure 1B illustrates that τ increases with decreasing k_c . A moment's reflection will reveal that these results are,

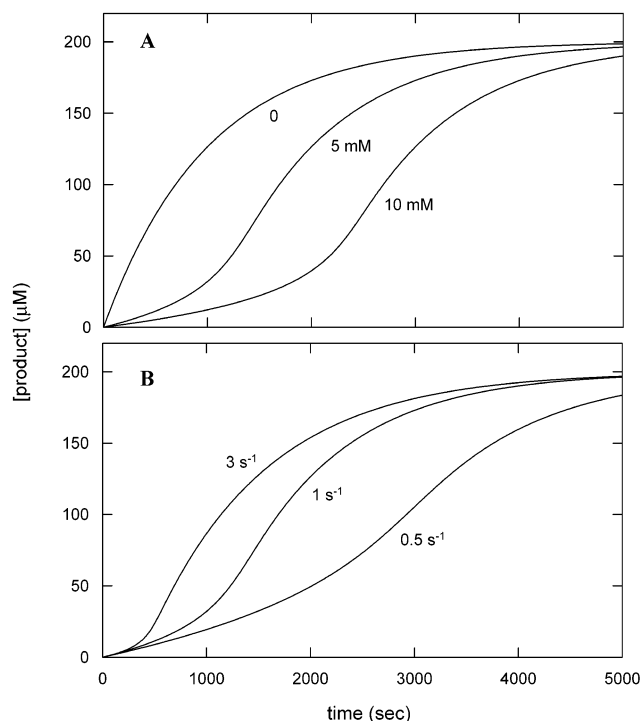


FIGURE 1: Simulations of the mechanism of Scheme 2 for reaction of the signal-generating substrate S* in the presence of competing, silent substrate S. (A) Parameters of simulation: $k_E^* = 200 \text{ M}^{-1} \text{ s}^{-1}$, $[S^*]_o = 200 \text{ } \mu\text{M}$, $k_c = 1 \text{ s}^{-1}$, $K_m = 500 \text{ } \mu\text{M}$, and $[E]_o = 5 \text{ } \mu\text{M}$. The initial concentration of S was varied as indicated. (B) Parameters of simulation: $k_E^* = 200 \text{ M}^{-1} \text{ s}^{-1}$, $[S^*]_o = 200 \text{ } \mu\text{M}$, $K_m = 500 \text{ } \mu\text{M}$, $[S]_o = 5 \text{ mM}$, and $[E]_o = 5 \text{ } \mu\text{M}$. k_c was varied as indicated.

of course, the expected results: relief from inhibition by silent substrate S occurs as S is turned over by enzyme and will occur sooner at lower initial concentrations of S as well as with more reactive silent substrates. (3) Perhaps most significantly, closer inspection of these simulations reveals that the ratio $[S]_o/\tau$ is a constant in Figure 1A and increases in direct proportion to k_c in Figure 1B. Note that $[S]_o/\tau$ has units of molar per second and, as we show below, is equal to V_{\max} or $k_c[E]_o$.

To demonstrate this last point, we start with the rate expressions of eqs 2 and 3, which describe the mechanism

$$\frac{d[P^*]}{dt} = -\frac{d[S^*]}{dt} = k_E^*[S^*][E] = k_E^*[S^*]\left\{\frac{[E]_o}{1 + [S]/K_m}\right\} \quad (2)$$

$$\frac{d[P]}{dt} = -\frac{d[S]}{dt} = k_c[ES] = k_c\left\{\frac{[E]_o}{1 + K_m/[S]}\right\} \quad (3)$$

of Scheme 2. An approximate expression for V_{\max} can be found by first expressing the lag phase duration, τ , in terms of the tangent line through the inflection point of a progress curve for the signal-generating substrate. Equation 4 shows τ defined this way as a function of the slope at the inflection point $[(d[S^*]/dt)_i]$ and the time to get to the inflection point (t_i).

$$\tau = \frac{[S^*]_o - [S^*]_i}{(d[S^*]/dt)_i} + t_i \quad (4)$$

Table 1: Accuracy of Equation 9 Determined from Analysis of Progress Curves Obtained by Integrating Equations 11 and 12

| α | β | % error ^a | α | β | % error ^a | α | β | % error ^a |
|----------|---------|----------------------|----------|---------|----------------------|----------|---------|----------------------|
| 5 | 5 | 91 | 10 | 5 | 41 | 20 | 5 | 21 |
| 5 | 10 | 51 | 10 | 10 | 24 | 20 | 10 | 13 |
| 5 | 15 | 38 | 10 | 15 | 18 | 20 | 15 | 9 |
| 5 | 20 | 30 | 10 | 20 | 12 | 20 | 20 | 8 |
| 5 | 25 | 26 | 10 | 25 | 14 | 20 | 25 | 6 |

^a The percent error is not the approximate expression of eq 10, but the exact relative error, $100(V_{\max, \text{estimate}} - V_{\max})/V_{\max}$.

Substitutions into eq 4 using the next three equations, which relate directly to Scheme 2 and the rate expressions above, give an approximate expression (eq 8) for the lag phase duration. The slope at the inflection point can be obtained directly from the rate expression of eq 2. At this point in the progress curve, the concentration of the silent substrate will be less than its K_m , so eq 5 can be used in place of the exact expression for the slope (the simulation results in Table 1 had lag phases with $[S]_i/K_m$ ranging from 0.1 to 0.002). Equation 6, obtained by integrating the simple Michaelis–Menten rate equation for the silent substrate, provides a useful expression for the time at the inflection point, and the relationship in eq 7 allows us to express part of the lag phase duration in terms of the signal substrate. This relationship is true because S* and S compete for the same pool of free enzyme. Integration of $d[S^*]/d[S]$ for the mechanism of Scheme 2 gives eq 7.

$$\left(\frac{d[S^*]}{dt}\right)_i \cong -k_E^*[S^*]_i[E]_o \quad (5)$$

$$t_i = \frac{[S]_o - [S]_i}{V_{\max}} - \frac{K_m}{V_{\max}} \ln\left(\frac{[S]_i}{[S]_o}\right) \quad (6)$$

$$\frac{K_m}{V_{\max}} \ln\left(\frac{[S]_i}{[S]_o}\right) = \frac{1}{k_E^*[E]_o} \ln\left(\frac{[S^*]_i}{[S^*]_o}\right) \quad (7)$$

With these substitutions into eq 4, the lag phase duration is approximated by eq 8. The term in braces will be near

$$\tau \cong \frac{[S]_o}{V_{\max}} - \frac{1}{k_E^*[E]_o} \left\{ \left(\frac{[S^*]_o}{[S^*]_i} - 1 \right) - \ln\left(\frac{[S^*]_o}{[S^*]_i}\right) \right\} \quad (8)$$

zero when $[S^*]_i \cong [S^*]_o$ (recall the property of logarithmic relationships that $\ln x \cong x - 1$ when x is near unity), leading to eq 9. More generally, V_{\max} estimated from eq 9 will always

$$V_{\max} \cong [S]_o/\tau \quad (9)$$

be greater than the true value by the approximate relative amount shown in eq 10. The approximation in eq 9 will be

% error in $V_{\max} \cong$

$$100\left(\frac{1}{\tau k_E^*[E]_o}\right) \left\{ \left(\frac{[S^*]_o}{[S^*]_i} - 1 \right) - \ln\left(\frac{[S^*]_o}{[S^*]_i}\right) \right\} \quad (10)$$

best when the inflection point in the progress curve occurs at low conversion of the signal substrate or, in cases with higher conversions, when the lag time is long relative to $1/k_E^*[E]_o$. High selective factors, k_E/k_E^* , will give good results by limiting consumption of the signal substrate during

the lag phase, and longer lag phases produced by higher initial concentrations of the silent substrate, relative to its K_m , will also improve the approximation.

The utility of eq 9 can be explored by recognizing that these two parameters, the selectivity factor and $[S]_o/K_m$, define the shape of the progress curve for the mechanism of Scheme 2. The rate equations (eqs 2 and 3) can be scaled using the following dimensionless variables: $x = [S^*]/[S]_o$, $y = [S]/[S]_o$, and $T = \tau k_E^*[E]_o$. With two new parameters defined as $\alpha = k_E/k_E^*$ and $\beta = [S]_o/K_m$, the transformed rate equations are eqs 11 and 12. Using a series of progress curves

$$dx/dT = -x/(1 + \beta y) \quad (11)$$

$$dy/dT = -\alpha y/(1 + \beta y) \quad (12)$$

generated by numerical integration of eqs 11 and 12, the accuracy of eq 9 can be mapped out for α and β (see Table 1). In the dimensionless coordinate system, V_{max} corresponds to α/β , and the inverse of the lag phase duration corresponds to the estimate of eq 9.

The error estimates of Table 1 decrease from a high of about 90%, when k_E/k_E^* and $[S]_o/K_m$ are both 5, to values that approach 6% as these defining ratios increase to 20 or 25. These trends are consistent with our intuition (see above) that the error in our estimate of V_{max} should decrease as these ratios increase. Even when k_E/k_E^* and $[S]_o/K_m$ are both small, an error of only a factor of 2 is acceptable for many more qualitative studies in enzymology.

Increased precision in our estimate of V_{max} can also be obtained by plotting τ as a function of $[S]_o$ (see Figure 4 for an example of this type of analysis). Such plots will be linear and have slopes equal to the reciprocal of V_{max} and are defined by eq 8, which include the error term in braces. Simulations demonstrate that this term is relatively insensitive to $[S]_o$; thus, slopes of these plots are better approximations of V_{max} than are estimates at single values of $[S]_o$.

A quantitative estimate of the accuracy of these slopes as measures of V_{max} can be obtained from the time derivative of eq 8, after using eq 7 to switch from the signal substrate to the silent substrate. The result, eq 13, shows the slope of

$$\frac{d\tau}{d[S]_o} = \frac{1}{V_{max}} - \frac{K_m}{[S]_o V_{max}} \left\{ \left(\frac{[S]_o}{[S]_i} \right)^{1/\alpha} - 1 \right\} \quad (13)$$

a plot of τ vs $[S]_o$ is nearly independent of $[S]_o$. Equation 13 can be further modified by replacing the silent substrate concentration at the inflection point, $[S]_i$, with the following expression, obtained by solving $d^2[S^*]/dt^2 = 0$ using the time derivative of eq 2 and appropriate substitutions from eq 3.

$$[S]_i = K_m/(\alpha - 1) \quad (14)$$

The final result, after using $\beta = [S]_o/K_m$, gives an equation for the slope used to demonstrate the accuracy of the method as is shown in Table 2.

$$\frac{d\tau}{d[S]_o} = \frac{1}{V_{max}} \left(1 - \frac{1}{\beta} \{ (\beta[\alpha - 1])^{1/\alpha} - 1 \} \right) \quad (15)$$

We see from this analysis that it should be possible to extract estimates of steady-state kinetic parameters for the enzymatic turnover of a silent substrate from progress curves

Table 2: Accuracy of the Inverse of Slopes^a of τ vs $[S]_o$ as Measures of V_{max}

| α | β | % error | α | β | % error | α | β | % error |
|----------|---------|---------|----------|---------|---------|----------|---------|---------|
| 5 | 5 | 20 | 10 | 5 | 10 | 20 | 5 | 5.4 |
| 5 | 10 | 12 | 10 | 10 | 6 | 20 | 10 | 3.1 |
| 5 | 15 | 9.2 | 10 | 15 | 4.4 | 20 | 15 | 2.2 |
| 5 | 20 | 7.5 | 10 | 20 | 3.5 | 20 | 20 | 1.8 |
| 5 | 25 | 6.4 | 10 | 25 | 3.0 | 20 | 25 | 1.5 |

^a The slopes predicted by eq 15 are time derivatives that vary slightly with $[S]_o$. The errors in the table represent the accuracy of the method using the instantaneous slopes at a single $[S]_o$ specified by β . To determine the slope experimentally, a plot like the one shown in Figure 4 is needed, effectively averaging the slopes at several substrate concentrations.

Table 3: Steady-State Kinetic Parameters for the α -Chymotrypsin-Catalyzed Hydrolysis of Suc-Ala-Phe-AlaNH₂ Determined by Competition with Suc-Ala-Phe-pNA^a

| [S] (mM) | k_E^* (mM ⁻¹ s ⁻¹) | K_m (mM) | k_c (s ⁻¹) | k_E (mM ⁻¹ s ⁻¹) |
|-------------|--|---------------|-----------------------------|--|
| 0 | 0.19 | | | |
| 0.6 | 0.18 | 0.39 | 1.1 | 2.8 |
| 1.1 | 0.23 | 0.34 | 0.58 | 1.7 |
| 2.2 | 0.23 | 0.35 | 0.77 | 2.2 |
| 4.5 | 0.23 | 0.37 | 0.86 | 2.3 |
| 9.0 | 0.19 | 0.55 | 1.0 | 1.8 |
| 18 | 0.19 | 0.61 | 1.0 | 1.7 |
| av | 0.21 ± 0.02 | 0.4 ± 0.1 | 0.9 ± 0.2 | 2.1 ± 0.4 |

^a Kinetic parameters were determined from the progress curves of Figure 1 as outlined in the text. Reaction progress curves were run with $[Suc-Ala-Phe-pNA]_o = 0.2$ mM, $[\alpha-CT]_o = 0.0047$ mM, and the indicated initial concentrations of Suc-Ala-Phe-AlaNH₂. Reaction conditions: 50 mM HEPES, 500 mM NaCl, and 10 mM CaCl₂, pH 8.0, at 30 °C.

for reaction of a signal-generating substrate that are run in the presence of the silent substrate. Furthermore, there appears to be at least two methods to perform this analysis. One method combines least-squares fitting with numerical integration of appropriate rate equations to analyze the progress curves, while the other method relies on direct graphical analysis in which K_m is the value of $[S]_o$ that reduces the control velocity by a factor of 2 (see eq 1) and V_{max} is shown to simply equal the ratio $[S]_o/\tau$. We now apply these methods to reactions of the serine protease, α -CT.

α -CT-Catalyzed Hydrolysis of Signal-Generating Substrate Suc-Ala-Phe-pNA. In previous studies (4), we demonstrated that, at pH 8.0 (50 mM HEPES, 500 mM NaCl, 10 mM CaCl₂) and 30 °C, α -CT hydrolyzes Suc-Ala-Phe-pNA to produce Suc-Ala-Phe and *p*-nitroaniline with steady-state rate constants: $k_c = 0.65$ s⁻¹, $K_m = 2.5$ mM, and $k_c/K_m = 240$ M⁻¹ s⁻¹.

This combination of high K_m and low reactivity makes this substrate an ideal signal-generating substrate for studies of α -CT's selectivity toward silent substrates. The high K_m is required to allow studies to be done at $[S^*] \ll K_m^*$ while still producing a large signal change ($\epsilon_{410} = 8800$ M⁻¹ cm⁻¹), and the low reactivity ensures that the silent substrate is entirely consumed before consumption of S^* .

In the studies to be described below, $[S^*]_o$ was set at 0.2 mM = $K_m^*/12$. On the plate reader that we used in these experiments, complete turnover of this substrate produces a ΔOD_{410} of about 0.9 (path length ~ 0.5 cm; $\epsilon_{410} = 8800$ M⁻¹ cm⁻¹). Since the resolution of this instrument is 0.01

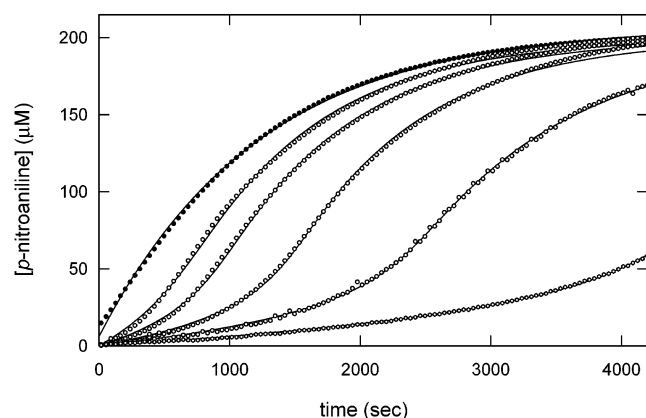


FIGURE 2: Progress curves for the α -CT-catalyzed hydrolysis of Suc-Ala-Phe-pNA in the presence of competing concentrations of Suc-Ala-Phe-AlaNH₂. Reaction progress curves were run with [Suc-Ala-Phe-pNA]₀ = 0.2 mM, [α -CT]₀ = 0.0047 mM, and [Suc-Ala-Phe-AlaNH₂]₀ = 0, 1.1, 2.3, 4.5, 9.0, and 18 mM (left to right in the figure). Solid lines through the data are based on simulations of the mechanism of Scheme 2 and the best fit parameters of Table 3. Reaction conditions: 50 mM HEPES, 500 mM NaCl, and 10 mM CaCl₂, pH 8.0, at 30 °C.

OD unit, we judged that a full deflection of 0.9 would provide progress curves of sufficient internal precision (see below).

Progress Curve Analysis for Reaction of Suc-Ala-Phe-pNA with α -CT in the Presence of Suc-Ala-Phe-AlaNH₂. Figure 2 contains reaction progress curves for the α -CT-catalyzed hydrolysis of Suc-Ala-Phe-pNA ($[S^*]_0 = 0.2 \text{ mM} \ll K_m^*$) in the presence of the competing, silent substrate Suc-Ala-Phe-AlaNH₂. At $[S]_0 = 0$, hydrolysis of S^* is pseudo first order with a k_{obs} value of $7.6 \times 10^{-4} \text{ s}^{-1}$ or $k_{\text{obs}}/[E]_0 = k_E^* = 190 \text{ M}^{-1} \text{ s}^{-1}$. As $[S]_0$ increases from 1.1 to 18 mM, a lag in the progress curve appears that can be seen to increase proportionately with $[S]_0$. This observation is consistent with theory (see above) and is a simple reflection of the additional time that is required to turn over a sufficient amount of S to relieve the inhibition of hydrolysis of S^* .

The curves of Figure 2 were fit to the mechanism of Scheme 2, and the results are summarized in Table 3. Note that this analysis includes a kinetic run conducted at $[S]_0 = 0.6 \text{ mM}$ which was not included in Figure 2 for the sake of clarity. The calculated kinetic parameters are independent of $[S]_0$ and thus support the kinetically simple mechanism of Scheme 2. Dependence of these parameters on $[S]_0$ would have signaled a complicating factor such as substrate inhibition or activation.

Graphical Analysis of the Progress Curves for Reaction of Suc-Ala-Phe-pNA with α -CT in the Presence of Suc-Ala-Phe-AlaNH₂. Figure 3 is a plot of initial velocities calculated from the progress curves of Figure 1 as a function of $[S]_0$. Since these curves were collected at $[S^*]_0 \ll K_m^*$, the $K_{i,\text{app}}$ determined from this dependence is equal to K_m (see eq 1). The K_m that was determined in this experiment is $0.51 \pm 0.03 \text{ mM}$ and equal to the K_m determined by analysis of the progress curves as outlined above.

Figure 4 illustrates how lag phases were graphically quantified and shows the linear dependence of these values on $[S]_0$. The slope of this dependence is $2.05 \times 10^5 \text{ s/M}$ and, as theory predicts, is equal to $1/V_{\text{max}} = 1/k_c[E]_0 = 4.9 \times 10^{-6} \text{ M/s}$. From this, and the $[E]_0$ of $4.7 \times 10^{-6} \text{ M}$, we calculate a k_c of 1.1 s^{-1} . Again, the value determined by

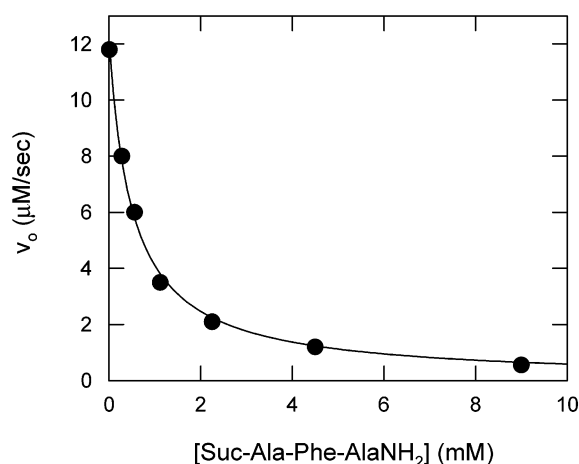


FIGURE 3: Substrate inhibition by Suc-Ala-Phe-AlaNH₂ of the α -CT-catalyzed hydrolysis of Suc-Ala-Phe-pNA. Initial velocities were calculated from the data of Figure 1 and plotted as a function of $[\text{Suc-Ala-Phe-AlaNH}_2]_0$. The solid line was drawn using eq 1 and the best fit parameters: $v_{\text{control}} = k_E^*[\alpha\text{-CT}]_0[S^*]_0 = 12.2 \pm 0.2 \text{ } \mu\text{M/s}$ and $K_m = 0.51 \pm 0.3 \text{ mM}$. Reaction conditions: 50 mM HEPES, 500 mM NaCl, and 0 mM CaCl₂, pH 8.0, at 30 °C.

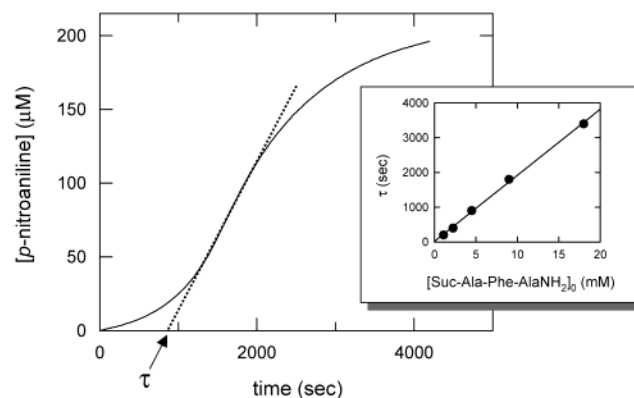


FIGURE 4: Graphical analysis of progress curves for the α -CT-catalyzed hydrolysis of Suc-Ala-Phe-pNA in the presence of competing concentrations of Suc-Ala-Phe-AlaNH₂. The data of this figure are taken from Figure 1 at $[\text{Suc-Ala-Phe-AlaNH}_2]_0 = 4.5 \text{ mM}$. The tangent to the curve was drawn manually and yields a τ value of 900 s. The inset is the substrate concentration dependence of τ determined in this way. The slope of this line is $190 \pm 4 \text{ s/mM}$, and the y-axis intercept is indistinguishable from zero (i.e., $13 \pm 40 \text{ s}$).

this direct method is in agreement with the k_c value determined by curve-fitting analysis.

Determination of the Steady-State Kinetic Parameters for the α -CT-Catalyzed Hydrolysis of Suc-Ala-Phe-AlaNH₂ by an HPLC-Based Method. To validate the methods just described, we determined steady-state kinetic parameters for the α -CT-catalyzed hydrolysis of Suc-Ala-Phe-AlaNH₂ by an HPLC-based method in which aliquots from a reaction solution are fractionated to separate products from unreacted substrate, and the latter is quantified and its time-dependent change analyzed. Figure 5 shows results from two independent experiments in which 5 mM Suc-Ala-Phe-AlaNH₂ was allowed to react with 1 μM α -CT, and the substrate peak from the chromatograms was integrated and plotted as a function of time. The line through the data was drawn using the integrated Michaelis–Menten and best fit parameters: $V_{\text{max}} = 1.16 \pm 0.05 \text{ } \mu\text{M/s}$ and $K_m = 0.48 \pm 0.13 \text{ mM}$. The results of multiple experiments at initial substrate concentra-

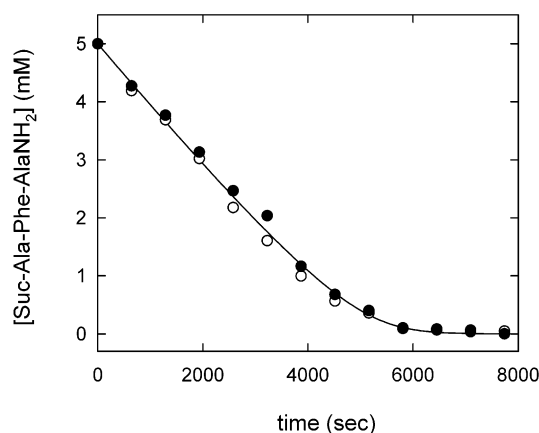


FIGURE 5: Progress curve analysis of the α -CT-catalyzed hydrolysis of Suc-Ala-Phe-AlaNH₂. Reaction progress was measured using the HPLC-based assay described in the text. The combined data from the two independent experiments of this figure (filled and empty circles) were fit to the integrated Michaelis–Menten equation with the following results: $V_{\max} = 1.16 \pm 0.05 \mu\text{M/s}$ and $K_m = 0.48 \pm 0.13 \text{ mM}$. Reaction progress curves were run with [Suc-Ala-Phe-AlaNH₂]₀ = 5 mM and [α -CT]₀ = 1.0 μM . Reaction conditions: 50 mM HEPES, 500 mM NaCl, and 10 mM CaCl₂, pH 8.0, at 30 °C.

Table 4: Steady-State Kinetic Parameters for the α -Chymotrypsin-Catalyzed Hydrolysis of Suc-Ala-Phe-AlaNH₂: HPLC-Based Assay and Progress Curve Method^a

| [S] (mM) | K_m (mM) | k_c (s ⁻¹) | k_E (mM ⁻¹ s ⁻¹) |
|-------------|-----------------|-----------------------------|--|
| 5 | 0.68 | 1.3 | 1.9 |
| 5 | 0.31 | 1.1 | 3.5 |
| 10 | 0.43 | 1.2 | 2.8 |
| 10 | 0.58 | 1.1 | 1.9 |
| av | 0.48 ± 0.19 | 1.2 ± 0.1 | 2.5 ± 0.8 |

^a Kinetic parameters were calculated by analysis of progress curves determined by the HPLC-based method described in the text. Reaction progress curves were run with [Suc-Ala-Phe-AlaNH₂]₀ = 5 mM and [α -CT]₀ = 1.0 μM . Reaction conditions: 50 mM HEPES, 500 mM NaCl, and 10 mM CaCl₂, pH 8.0, at 30 °C.

tions of 5 and 10 mM are summarized in Table 4. The agreement between these values and those determined by the competition methods validates the latter.

Summary and Conclusions. In this paper, we presented a new method for determining steady-state kinetic parameters for enzyme-catalyzed reactions of substrates whose turnover is not accompanied by a change in some physicochemical property that can easily be followed over time. While this new method was applied to reaction of α -CT, a serine protease, it can just as easily be used to determine the kinetics of silent substrates for any number of enzymes. All that is required is that certain conditions be met: (1) Signal-generating substrate S* must possess a K_m^* value that is large enough to ensure that kinetic studies can be done at $[S^*] \ll K_m^*$. (2) S* must also possess a k_c^* value that is small to ensure that S* is not depleted prior to full consumption of

the silent substrate. Thus, k_c must be greater than k_c^* . (3) To accurately determine K_m and k_c for the silent substrate, it must be possible to work at concentrations of S that are greater than $3 \times K_m$. This requires substrates of sufficient solubility to be used at the necessary concentrations.

One can imagine a number of kinetic situations that might confound the application of this technique. We already mentioned substrate inhibition and activation and noted that the presence of these would be reflected in an anomalous $[S]_0$ dependence of k_c and K_m . Complications in interpretation might also occur if the substrate can bind to free enzyme in more than a single mode; this is particularly relevant for protein and long peptidic substrates. One example of this phenomenon is nonproductive binding in which the complex formed from the binding of substrate to enzyme is not kinetically competent. This additional binding mode has the effect of lowering both k_c and K_m for the silent substrate but would go undetected in the analysis of our progress curves. On the other hand, if more than a single kinetically competent complex is formed and if the products of these reactions are themselves substrates for further reaction, progress curves generated using this method would have complex shapes that would resist simple analysis.

Finally, this method can also be applied to the analysis of enzyme inhibition and should be especially useful in situations where the inhibitor binds to an “exo site”, that is, a site on the enzyme surface that is at some distance from and distinct from the active site (5–7). For example, in cases where a protease inhibitor binds at a site that blocks interaction with protein substrates but does not block interaction with standard, peptidic chromophoric substrates, this method should reveal no change in τ but an increase in K_m that is consistent with competitive inhibition of the hydrolysis of the protein substrate. In contrast, such an inhibitor may have little or no effect on the hydrolysis of small, peptidic substrates. Clearly, inhibition of enzymes other than proteases that work on macromolecular substrates could be analyzed in this way.

REFERENCES

1. Fersht, A. R. (1999) in *Structure and Mechanism in Protein Science*, pp 191–199, W. H. Freeman, New York.
2. Copeland, R. A. (2000) in *Enzymes—A Practical Introduction to Structure, Mechanism, and Data Analysis*, pp 188–223, John Wiley & Sons, New York.
3. Harrison, R. K., Teahan, J., and Stein, R. L. (1989) *Anal. Biochem.* 80, 110–113.
4. Case, A., and Stein, R. L. (2003) *Biochemistry* 42, 3335–3348.
5. Roberge, M., Santell, L., Dennis, M. S., Eigenbrot, C., Dwyer, M. A., and Lazarus, R. A. (2001) *Biochemistry* 40, 9522–9531.
6. Monteiro, R. Q., Raposo, J. G., Wisner, A., Guimaraes, J. A., Bon, C., and Zingali, R. B. (1999) *Biochem. Biophys. Res. Commun.* 262, 819–822.
7. Fuentes-Prior, P., Noeske-Jungblut, C., Donner, P., Schleuning, W. D., Huber, R., and Bode, W. (1997) *Proc. Natl. Acad. Sci. U.S.A.* 94, 11845–11850.

BI0207162